Electrochemical properties of P2-phase Na0.74CoO2 compounds as cathode material for rechargeable sodium-ion batteries

ARTICLE *in* ELECTROCHIMICA ACTA · JANUARY 2013

Impact Factor: 4.5 · DOI: 10.1016/j.electacta.2012.09.058

5 AUTHORS, INCLUDING:

Yong-Ning Zhou
Brookhaven National Laboratory
32 PUBLICATIONS **287** CITATIONS
SEE PROFILE

Qian Sun
The University of Western Ontario
39 PUBLICATIONS **600** CITATIONS
SEE PROFILE

Electrochimica Acta 87 (2013) 388–393

Contents lists available at SciVerse ScienceDirect

Electrochimica Acta

journal homepage: www.elsevier.com/locate/electacta

Electrochemical properties of P2-phase $Na_{0.74}CoO_2$ compounds as cathode material for rechargeable sodium-ion batteries

J.J. Ding[a], Y.N. Zhou[b], Q. Sun[a], X.Q. Yu[b], X.Q. Yang[b], Z.W. Fu[a,*]

[a] Shanghai Key Laboratory of Molecular Catalysts and Innovative Materials, Department of Chemistry & Laser Chemistry, Fudan University, Shanghai 200433, China
[b] Brookhaven National Laboratory, Upton, NY 11973, USA

ARTICLE INFO

Article history:
Received 13 July 2012
Received in revised form
18 September 2012
Accepted 20 September 2012
Available online 26 September 2012

Keywords:
Sodium ion battery
Sodium cobalt oxides
Cathode material

ABSTRACT

P2-phase $Na_{0.74}CoO_2$ cathode material prepared by a solid-state method exhibits the specific discharge capacity of 107 mAh g^{-1} at 0.1 C with good cycling performance for rechargeable sodium ion batteries. The voltage polarization between charging and discharging at 0.1 C rate is about 150–250 mV and the coulombic efficiency in each cycle is about 89%. The expansion and compression in *c*-axis of the Na_xCoO_2 unit cell during the Na intercalation/deintercalation is revealed by *ex situ* XRD. XPS and *in situ* XAS data directly confirm that deintercalation/intercalation of Na ions from/into the layered structure proceeds with the Co^{3+}/Co^{4+} redox reaction.

1. Introduction

In response to the great interest in searching new advanced batteries for electric vehicles (EV) and smart grids, sodium ion secondary batteries (SIBs) have drawn wide attention due to the abundant resources and low costs [1–4]. Over the last decades much efforts have been devoted to the development of layered transition metal oxides such as Na_xMO_2 (M = Co, Ni, Mn, Cr, Fe) as cathode active materials [5–13]. Among them, Na_xCoO_2 shows high reversible capacity and good cyclability. The electrochemical intercalation or deintercalation of sodium in layered Na_xCoO_2 oxides and the four phases of Na_xCoO_2 with different structures (in the composition range of $0.5 \leq x \leq 1$) had been studied as positive electrode materials by Braconnier et al. in 1980s [9]. Shacklette et al. examined the electrochemical performances of $Na_{0.67}CoO_2$ with O3, O′3, P3, P2 phases and indicated that the P2-phase offers better cycle life and better energy efficiency [5]. Huang et al. reported that the hexagonal Na_xCoO_2 has three structure types by neutron powder diffraction [14]. Various P2 phases, with *x* ranging approximately from 0.6 to 0.75, had been studied by variable-temperature ^{23}Na magic angle spinning (MAS) NMR [15]. Recently, Berthelot et al. clarified a series of single-phase or two phase transition of the P2-phase $Na_{0.74}CoO_2$ by using *in situ* XRD technique [16]. Although many of the insertion systems and the structure of sodium cobalt oxides have been characterized [17–23], not many studies on the discharge capacity and the rate capability of various sodium cobalt oxides have been reported. In the present study, P2-phase $Na_{0.74}CoO_2$ powder was synthesized by a solid-state reaction method. Its electrochemical behavior and charge transfer mechanism were studied to elucidate the nature of the electrochemical intercalation/deintercalation of Na_xCoO_2 with sodium for the development of SIBs.

2. Experimental

2.1. $Na_{0.74}CoO_2$ powder synthesis

$Na_{0.74}CoO_2$ was synthesized by solid-state reaction at high temperature. The mixtures of Na_2CO_3 (Na_2CO_3 was analytical reagent and purchased from Wenmin Bio-Chemistry Science Co., Ltd., China) and $CoCO_3$ ($CoCO_3$ was 99% pure and from Alfa Aesar, Tianjin, China) powders in a 1:2 mol ratio were well grounded by ball milling and heated at 800 °C for 12 h in air. The $Na_{0.74}CoO_2$ powder was successfully obtained.

2.2. Physical characterization

Inductively coupled plasma (ICP) emission spectroscopy (P-4010, Hitachi Co., Japan) was used to measure the chemical composition of $Na_{0.74}CoO_2$ powder. XRD patterns of samples were recorded by a Rigaku/max-C diffractometer with Cu Kα radiation (1.5406 Å) in the 2θ scale between 10 and 70° at a scan rate of 4°/min. The morphology of the synthesized powders was investigated by SEM (Cambridge S-360) with the operating voltage of

* Corresponding author. Tel.: +86 21 65642522; fax: +86 21 65102777.
E-mail addresses: zwfu@fudan.edu.cn, zhengwen@sh163.net (Z.W. Fu).

0013-4686/$ – see front matter © 2012 Elsevier Ltd. All rights reserved.
http://dx.doi.org/10.1016/j.electacta.2012.09.058

25 kV. High resolution transmission electron microscopy (HRTEM) and selected area electron diffraction (SAED) measurements were performed on a 200 kV side entry JEOL 2010TEM. XPS data were collected on a Perkin-Elmer PHI 5000C ECSA system with monochromatic Al Kα (1486.6 eV) irradiation.

In situ Co K-edge X-ray absorption spectra (XAS) were collected in transmission mode at beamline X18A at the National Synchrotron Light Source (NSLS) at Brookhaven National Laboratory (BNL) using a Si(1 1 1) double-crystal monochromator. The monochromator was detuned to 35–45% of its original intensity to eliminate the high order harmonics. Energy calibration was carried out using the first inflection point of the spectrum of Co metal foil as a reference (Co K-edge = 7709 eV). Reference spectrum was simultaneously collected for each *in situ* spectrum using Co metal foil.

2.3. Electrochemical tests

The electrodes were made of the active material, the super P carbon and the poly (vinylidene fluoride) in a weight ratio of 80:10:10. To evaluate electrochemical performance, the cells were constructed using the $Na_{0.74}CoO_2$ as cathode, a sodium metal as anode and the electrolyte of 1 M $NaPF_6$ or 1 M $NaClO_4$ in a nonaqueous solution of ethylene carbonate (EC) and dimethyl carbonate (DMC) with a volume ratio of 1:1. The model cells constructed of stainless steel and Teflon™ were assembled in an Ar-filled glove box. A Celgard 2400 polyethylene was used as a separator. Charge–discharge measurements were performed at room temperature with a Land BT 1-40 batteries test system. The cells were cycled between 2.0 and 3.8 V *vs.* Na/Na^+ at constant current density at different rates for the discharge and charge processes. The active material loading amount was 5.68 mg cm^{-2}. Cyclic voltammetry (CV) test was carried out at a scan rate of 0.1 mV s^{-1} between 2.0 and 3.8 V on a CHI660A electrochemical working station (CHI Instruments, TN) with a three-electrode system, in which the $Na_{0.74}CoO_2$ was used as a working electrode with two sodium sheets as a counter electrode and reference electrode, respectively. In a three electrode system, the reference electrode can avoid tiny potential change. The model cells were dismantled in an Ar-filled glove box and the electrodes were rinsed in anhydrous, dimethyl carbonate (DMC) to eliminate residual salts. To avoid the exposure to oxygen or water in air, the samples were sealed up in a quartz container for *ex situ* measurements.

3. Results and discussion

3.1. Characterization of $Na_{0.74}CoO_2$ powder

The XRD pattern of the synthesized $Na_{0.74}CoO_2$ powders is presented in Fig. 1. The diffraction peaks at $2\theta = 16.38^\circ$, 33.00°, 36.65°, 40.32°, 44.62°, 50.08°, 63.83°, 65.91°, 68.48° of the powder could be well assigned to the reflection of crystal structure type of P2-phase $Na_{0.74}CoO_2$ with space group $P6_{3/mmc}$ (JCPDS card no. 87-0274). The lattice parameters calculated from the XRD pattern were: $a = 2.823$ Å, $c = 10.815$ Å. As shown in the inset of Fig. 1, P2-Na_xCoO_2 displays a structure with an ABBA stacking sequence for edge-sharing octahedral, CoO_6 layers. Octahedral and trigonal prismatic sites are occupied by Co and Na ions, respectively. In this structure, the Na^+ ions are distributed in two distinct prismatic sites labeled Na(1) and Na(2) in previous literature: Na(1) shares only faces whereas Na(2) shares only edges with surrounding CoO_6 octahedra [15,17].

Both HRTEM and SEM techniques were used to gain further insight into the structure and morphological aspects of $Na_{0.74}CoO_2$ powder. As shown in Fig. 2(a), the clear crystal lattices with a

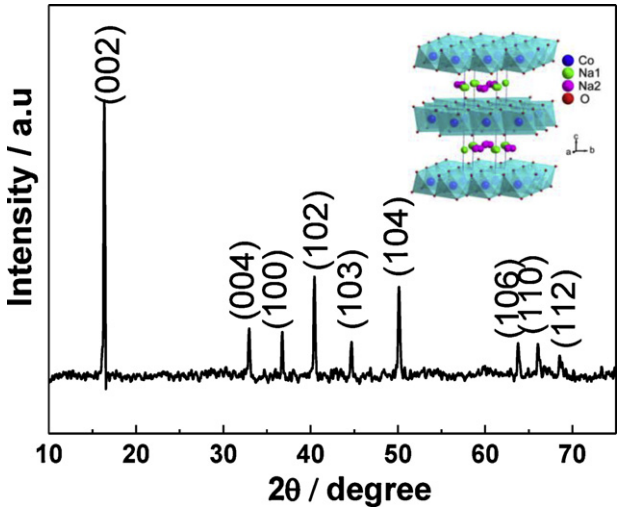

Fig. 1. XRD patterns of the pristine $Na_{0.74}CoO_2$ compound. Major diffraction circles in XRD patterns are labeled with *hkl* notation of P2-$Na_{0.74}CoO_2$ (JCPDS card no. 87-0274). The lamellar structure of P2-$Na_{0.74}CoO_2$ (right) is shown as an inset.

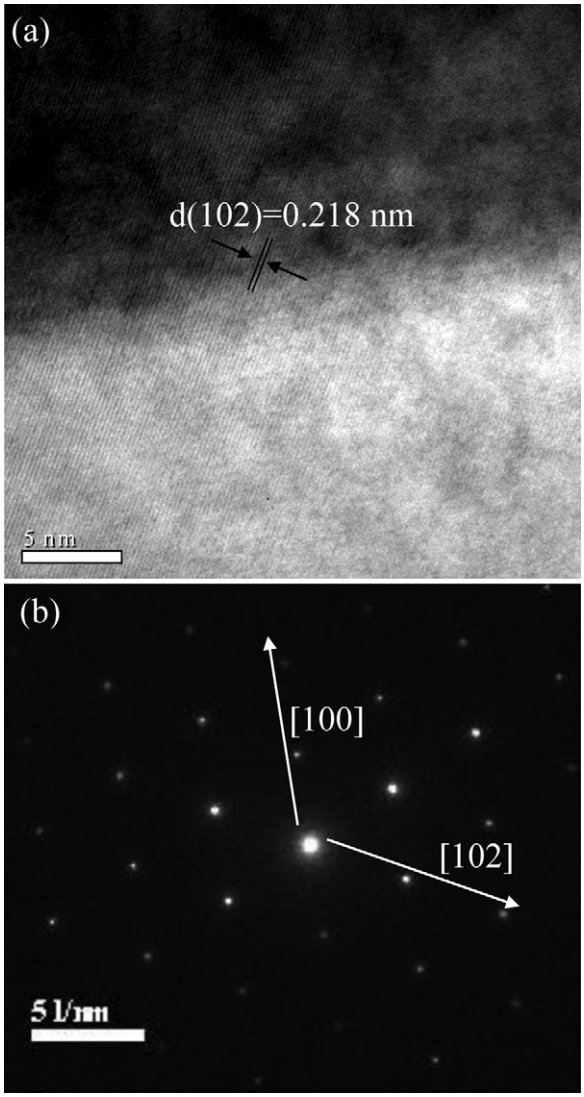

Fig. 2. (a) The high resolution TEM and (b) SAED patterns of the pristine compound.

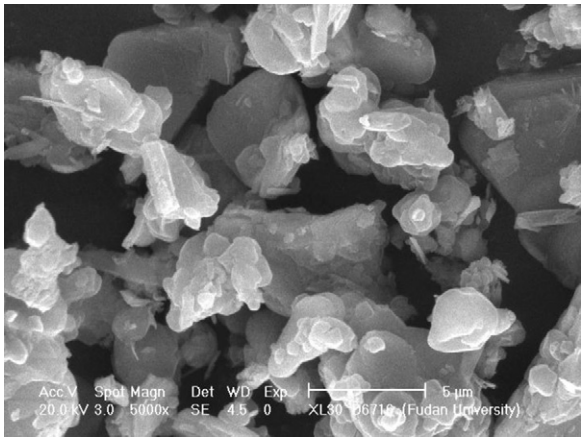

Fig. 3. The SEM images of the pristine compound.

d-spacing of 2.184 Å corresponding to the (1 0 2) plane of $Na_{0.74}CoO_2$ are observed. Fig. 2(b) shows the SAED pattern of this phase, which was taken from [0 1 0] projection. Clear two-dimension diffraction spots along [1 0 0] and [1 0 2] axis can be observed. This result is in good agreement with the XRD pattern. Fig. 3 shows the SEM image of the pristine $Na_{0.74}CoO_2$ powders. The images indicate a disordered morphology composed individual particles in the range of 0.2–0.5 μm. The small particles fused together to form micro-sized irregular agglomerates in the size range 1–5 μm.

3.2. Electrochemical properties

The electrochemical performance of the P2-phase $Na_{0.74}CoO_2$ in different electrolytes has been studied. Fig. 4(a) shows the charge/discharge curves of P2-phase $Na_{0.74}CoO_2$/$NaPF_6$/Na cell. The cell was cycled between 2.0 V and 3.8 V at a current density of 0.1 C. The cell exhibits an open circuit voltage (OCV) of 2.71 V. The first sodium deintercalation curve shows four voltage plateaus at 2.72 V, 3.00 V, 3.30 V, and 3.60 V. For the initial discharging profiles, there are eight plateaus as shown in the figure. Apparently, Na deintercalation and intercalation cycled between 2.0 V and 3.8 V undergoes complicated series of successively phase transitions, which have been investigated by *in situ* XRD measurement [16]. Huang et al. reported that in the H1 phase, the Na ion content is $0.3 < x < 0.75$, while in the H2 and H3 phase, the Na ion content is $0.76 < x < 0.82$ and $x = 1$, respectively [14]. The initial charge and discharge capacities are found to be about 55.7 mAh g^{-1} and 107.0 mAh g^{-1}, respectively corresponding to the formation of $Na_{0.50}CoO_2$ and $Na_{0.93}CoO_2$ by presuming that all charge passed at the electrode was compensated by increase or decrease in valence of Co with Na^+ extraction or insertion. The voltage polarization between the charging and discharging voltage profiles is about 150–250 mV, much larger than that of Li/$LiCoO_2$ battery [24]. Fig. 4(b) shows the charge/discharge curves of P2-phase $Na_{0.74}CoO_2$/$NaClO_4$/Na cell. The cell was cycled between 2.0 V and 3.8 V at a current density of 0.05 C. The initial charge and discharge capacities are found to be about 54.86 mAh g^{-1} and 110.2 mAh g^{-1} respectively. The electrochemical performance of $Na_{0.74}CoO_2$ in $NaClO_4$ electrolyte is similar with that in $NaPF_6$ electrolyte. However, the capacity retention is not as good as that in $NaPF_6$ electrolyte. The discharge capacity in the 40th cycle is 57.53 mAh g^{-1}, which is only 52.2% of the initial capacity. The coulombic efficiency of the both cells is shown in Fig. 4(c). $Na_{0.74}CoO_2$ in $NaPF_6$ electrolyte exhibits better cycling performance but lower coulombic efficiency than that in $NaClO_4$ electrolyte. Tirado's group reported that $NaPF_6$ was chosen instead of $NaClO_4$ in order to avoid safety

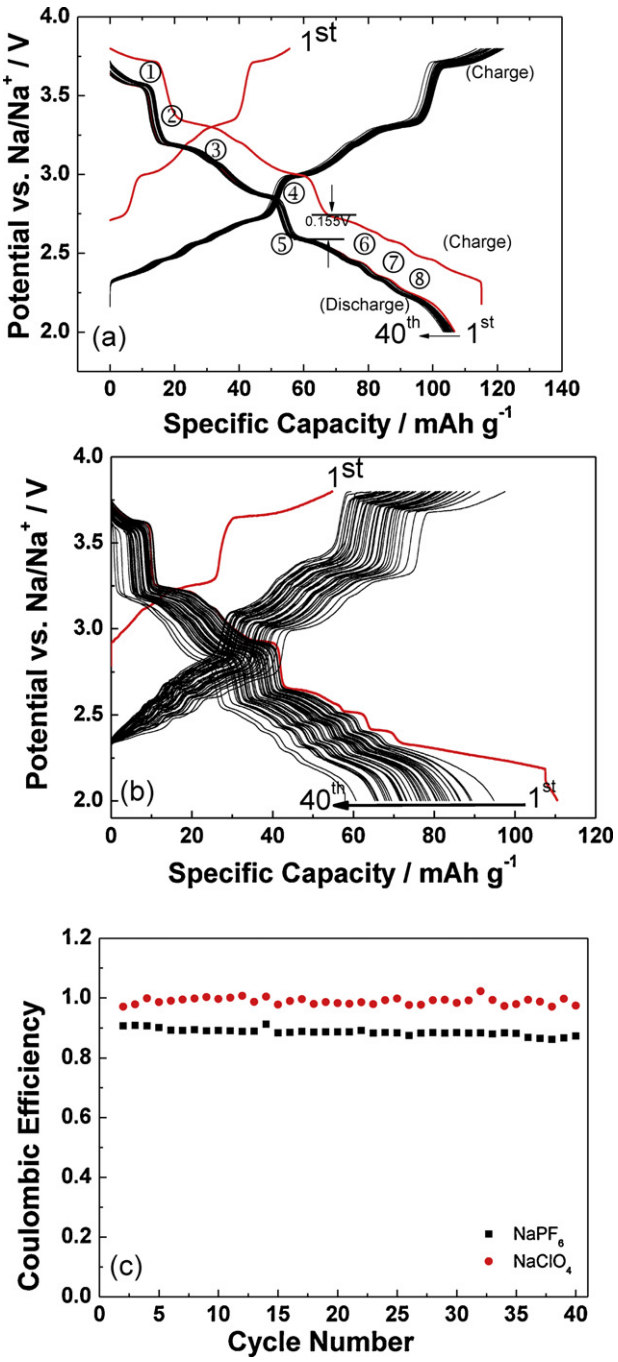

Fig. 4. (a) Galvanostatic curves of P2-$Na_{0.74}CoO_2$/$NaPF_6$/Na cells at the current rates of 0.1 C; (b) galvanostatic curves of P2-$Na_{0.74}CoO_2$/$NaClO_4$/Na cells at the current rates of 0.05 C, and (c) coulombic efficiency of the cells as a function of cycle numbers.

problems associated to the use of perchlorates [25]. A comparative study has been carried out on diverse electrolyte formulations with different sodium salts and solvents or solvent mixtures by Ponrouch et al. [26]. They reported that $NaPF_6$ in EC:PC fulfills at present all the necessary conditions to be adopted as a standard electrolyte in sodium ion batteries. These results show that $NaPF_6$ is a good sodium ion electrolyte.

The specific capacity and coulombic efficiency as functions of cycle number are shown in Fig. 5 at various current rates from 0.1 to 2 C. A reversible discharge capacity of 103.0 mAh g^{-1} after the initial 40th cycles is obtained. The capacity loss is less than 0.1% per cycle in initial 40th cycles. The coulombic efficiency in the forty cycles could be remained above 89%. A specific discharge capacity around

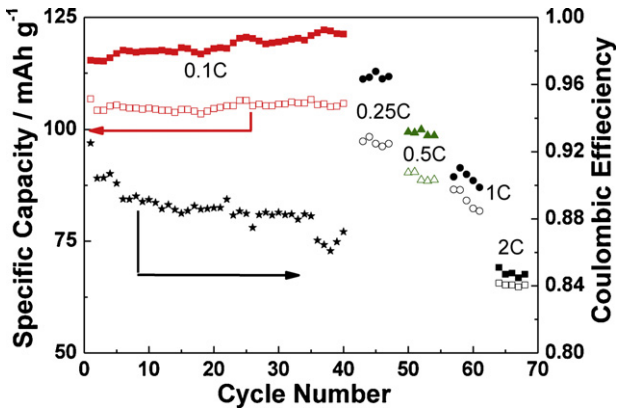

Fig. 5. The corresponding coulombic efficiency and specific discharge and charge capacities of the P2-$Na_{0.74}CoO_2$/$NaPF_6$/Na cells at the various current rates of 0.1 C, 0.25 C, 0.5 C, 1 C and 2 C as a function of cycle numbers, the charge capacities and discharge capacities are represented by solid and hollow symbol, respectively.

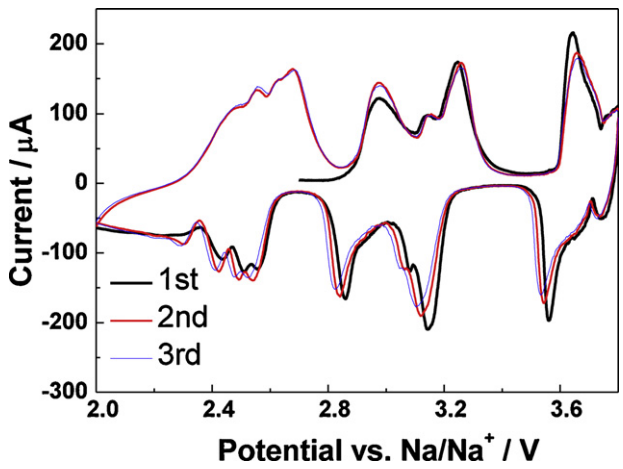

Fig. 6. Cyclic voltammogram for P2-$Na_{0.74}CoO_2$/$NaPF_6$/Na cell between 2.0 and 3.8 V at scan rate of 0.1 mV s^{-1}.

96 mAh g^{-1} is obtained at a rate of 0.25 C. The specific reversible discharge capacities reduce gradually to 89, 83 and 65 mAh g^{-1} at rates of 0.5 C, 1 C and 2 C, respectively. The capacity retention at the current density of 2 C is about 68% compared to the capacity at 0.25 C. The discharging capacity is in good agreement with that of Berthelot et al. [16].

Cyclic voltammogram curves of the Na/$NaPF_6$/P2-$Na_{0.74}CoO_2$ cell between 2.0 and 3.8 V at the scan rate of 0.1 mV s^{-1} is shown in Fig. 6. During the first cycle, four cathodic peaks were found at 2.97 V, 3.14 V, 3.24 V and 3.64 V. In the second cycle, there are eight distinct cathodic peaks at 2.46 V, 2.56 V, 2.62 V, 2.68 V, 2.98 V, 3.14 V, 3.26 V and 3.66 V, while eight corresponding anodic peaks are observed at 2.29 V, 2.41 V, 2.47 V, 2.52 V, 2.82 V, 3.05 V, 3.10 V and 3.53 V, respectively. These CV data are in good agreement with the discharge/charge curves of P2-$Na_{0.74}CoO_2$/Na cell in Fig. 4.

3.3. Sodium reaction mechanism

To further study the structure change of P2-Na_xCoO_2 after charge and discharge, the XRD and XPS are employed. The XRD patterns of the as-prepared electrode shown in Fig. 7(a) indicates that some structure changes of P2-Na_xCoO_2 occur during the fabrication of the electrode even before the electrochemical cycling. Comparing with the XRD patterns of P2-Na_xCoO_2 powders in Fig. 1, the diffraction peaks in Fig. 7(a) at $2\theta = 36.65^\circ$, 68.48°, 69.11° disappear and the peak at $2\theta = 33^\circ$ becomes relatively stronger. The XRD patterns after first charge and discharge are presented in Fig. 7(b) and (c), respectively. After the electrode is charged to 3.8 V, it can be observed that the peak at 16.38° of P2-Na_xCoO_2 (Fig. 7(a)) shifts to 15.93° as shown in Fig. 7(b). When the electrode is discharged to 2.0 V, this (0 0 2) peak of P2-Na_xCoO_2 structure shifts back to 16.58° (Fig. 7(c)). The *c*-lattice parameter for the pristine powder sample, for the electrode after the first charge to 3.8 V and for the electrode after the first discharge to 2.0 V are calculated to be 10.815, 11.118, 10.685 Å respectively. Na intercalation/deintercalation into/from the lamellar structure P2-Na_xCoO_2 should be responsible for the changes of the *c*-lattice parameter. The *c*-lattice parameter becomes larger with decreasing sodium content. Such variation is similar to the (0 0 8) peak variation of P2-$Na_{0.74}CoO_2$ [16]. It is believed that the expansion in the *c*-axis direction should be attributed to an increase in electrostatic repulsion from the negatively charged oxygen–oxygen interactions of CoO_2 layers with the removal of

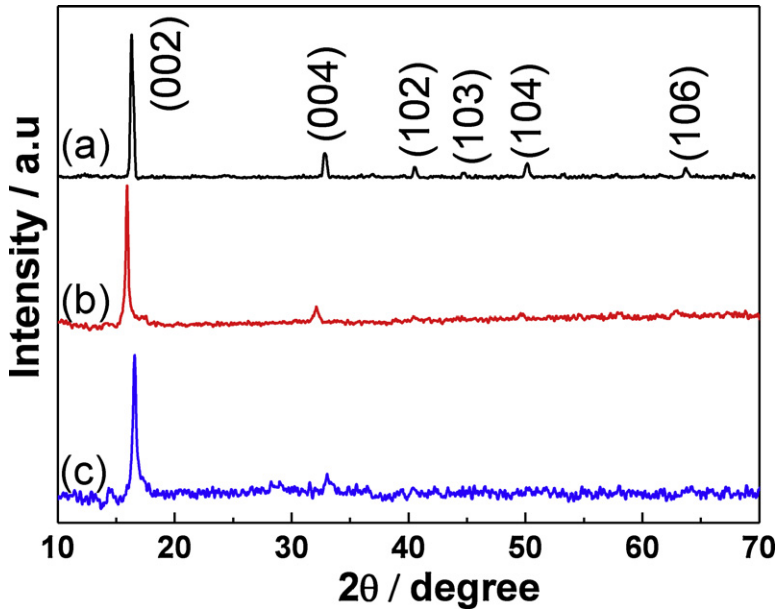

Fig. 7. XRD patterns of (a) the fresh electrode; (b) the electrode after the first charging to 3.8 V; (c) the electrode after the first discharging to 2.0 V.

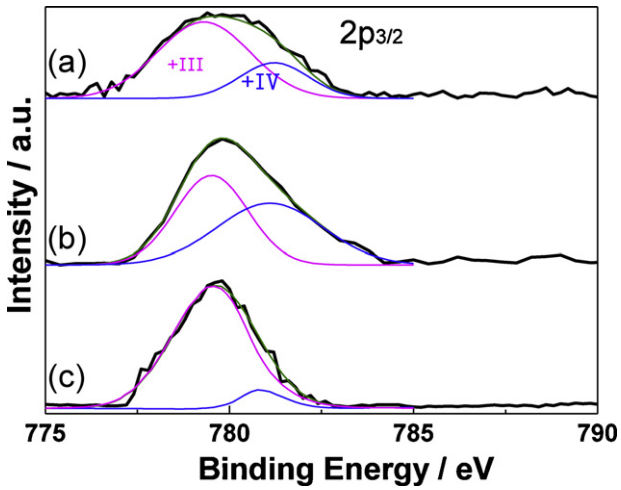

Fig. 8. Co $2p_{3/2}$ XPS spectra of (a) the pristine powder; (b) the electrode after the first charging to 3.8 V; (c) the electrode after the first discharging to 2.0 V.

sodium. It can be estimated that Na intercalation/deintercalation leads to about 4% contraction and expansion *along* *c*-axis. It should be noted that only two diffraction peaks of the (0 0 2) and (0 0 4) reflections of P2-Na_xCoO_2 in XRD patterns of those electrodes after the Na intercalation/deintercalation processes (as shown in Fig. 7(b) and (c)) are observed, indicating a strong preferred *c*-axis (0 0 2) out-of-plane orientation. The same phenomenon was also noted by Delmas' group [16]. They noted that preferential orientation of the active material during electrode material preparation enhanced the (0 0 l) diffraction peaks and lowered the others.

Co $2p_{3/2}$ XPS spectra of the pristine powder, the electrode after the first charge to 3.8 V and the electrode after the first discharging to 2.0 V are shown in Fig. 8. All measured solid curves in Fig. 8 could be deconvoluted into two component peaks at 779.3 eV and 781.1 eV with energy separation of 1.8 eV. According to previous studies, they can be attributed to the Co $2p_{3/2}$ binding energy for Co^{3+} and Co^{4+}, respectively [27]. As shown in Fig. 8(a), the relative intensity (area) ratio of the peak at 779.3 eV to the peak at 781.1 eV is about 0.74:0.26, indicating that the pristine powder has a formula of $Na_{0.74}CoO_2$. This is consistent with ICP and XRD data.

After the electrode charging to 3.8 V, the Co $2p_{3/2}$ spectrum is different from that of the pristine powder and the relative peak intensity ratio of the peak at 779.34 eV to the peak at 781.1 eV reduces to about 0.50:0.50, which suggest that Co^{3+} is oxidized to higher valence of Co^{4+} during the charge process. When the electrode is discharged to 2.0 V, the relative intensity ratio of the peak at 779.34 eV to the peak at 781.1 eV is about 0.93:0.07, which means that most Co^{4+} ions are reduced to Co^{3+}.

In order to further investigate the mechanism of Na_xCoO_2, synchrotron based *in situ* XAS was used to monitor the detailed structural changes in the electrode material during Na ion extraction. In general, the position of the absorption edge provide information about the oxidation state of the atoms being probed, while the shape of the K-edge XAS of the transition metal oxides provides unique information about the site symmetry and the nature of the bonding with surrounding ligands. Fig. 9(a) shows the first charging curve for the *in situ* cell with a $Na_{0.74}CoO_2$ cathode when charged at a current rate of C/10. The numbers corresponding to XAS scans in Fig. 9(b) and (c) are marked on the charging curve in Fig. 9(a). The *in situ* Co K-edge normalized X-ray absorption near-edge structure (XANES) spectra and the corresponding

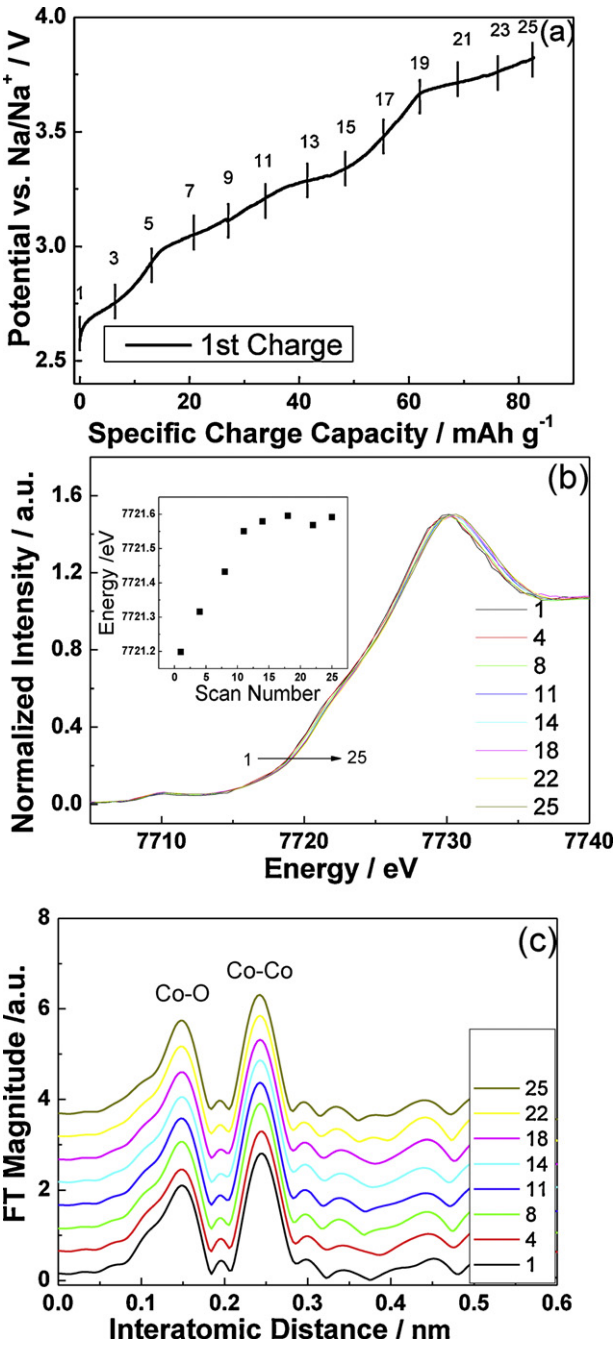

Fig. 9. (a) The first charging curves of a $Na/Na_{0.74}CoO_2$ cell at a current rate of C/10 from 2.6 to 3.8 V; (b) *in situ* Co K-edge XANES spectra of Na_xCoO_2 during the charging process and the corresponding energy edge position is shown in the inset; (c) the Fourier transform of the Co K-edge EXAFS spectra at different charge states.

edge position of the first charging process at different charge states are shown in Fig. 9(b). The Co K-edge edge position in the inset of Fig. 9(b) shows a progression of the entire pattern from lower energy to higher energy as a function of the decreased Na content, indicating the oxidation of Co^{3+} toward Co^{4+}.

The local structure of the Co is obtained from EXAFS measurements. As shown in Fig. 9(c), the first peak at ~1.48 Å corresponds to the Co—O bond. The gradual reduction of Co—O bond length from 1.51 Å at pristine state to 1.48 Å at charged state is seen in Fig. 9(c) during charge process. The variation of the interatomic distance is closely related to the change in the valence state of the transition metal. Deb's [28] reported that the outermost

electronic configuration of Co^{3+}/Co^{4+} can be represented as $t^6_{2g}e^0_g/t^5_{2g}e^0_g$ and the change in energy in Co^{3+}/Co^{4+} is very small during the oxidation reaction of the charging process because the change takes place only in the t_{2g} degenerate set, which results in a very small change in the ionic radius. The second peak at ~2.44 Å corresponds to a Co—Co interaction. It can be seen that at the Co—Co bond length has no obviously shift upon delithiation. This is similar as the behavior observed in $LiCoO_2$ system [29].

The XPS and XAS results provide strong evidences on that the deintercalation/intercalation of Na ions from/into the layered structure proceeds with the Co^{3+}/Co^{4+} redox reaction. Combining with the discharge/charge data as shown in Fig. 4, it can be found that the Co^{3+}/Co^{4+} redox couple undergoing valence conversion on the anionic network of oxygen atom layer assures the specific capacities of Na_xCoO_2.

4. Conclusions

The P2-$Na_{0.74}CoO_2$ as cathode material for sodium-ion batteries has been successfully synthesized by a solid-state reaction in air. It exhibits better electrochemical performance in $NaPF_6$ than $NaClO_4$. A reversible capacity of 107 mAh g^{-1} is obtained in the voltage range of 2.0–3.8 V with the capacity fading of 0.1% per cycle for the first 40 cycles in $NaPF_6$ electrolyte. However, it suffers from high voltage polarization of ~150–250 mV at 0.1 C and low coulombic efficiency of 89%. The intercalation/deintercalation of Na ions into/from $Na_{0.74}CoO_2$ leads to the lattice contraction/expansion along *c* axis and the Co^{3+}/Co^{4+} redox reaction.

Acknowledgements

This work was financially supported by Science & Technology Commission of Shanghai Municipality (08DZ2270500 and 11JC1400500) and 973 Program (No. 2011CB933300) of China. The work at Brookhaven National Laboratory was supported by the U.S. Department of Energy, the Assistant Secretary for Energy Efficiency and Renewable Energy, Office of Vehicle Technologies, under Contract Number DEAC02-98CH10886.

References

[1] B.L. Ells, W.R.M. Makahnouk, Y. Makimura, K. Toghill, L.F. Nazar, A multifunctional 3.5 V iron-based phosphate cathode for rechargeable batteries, Nature Materials 6 (2007) 749.
[2] J.M. Tarascon, Key challenges in future Li-battery research, Philosophical Transactions of the Royal Society 368 (2010) 3227.
[3] S.P. Ong, V.L. Chevrier, G. Hautier, A. Jain, C. Moore, S. Kim, X. Ma, G. Ceder, Voltage, stability and diffusion barrier differences between sodium-ion and lithium-ion intercalation materials, Energy and Environmental Science 4 (2011) 3680.
[4] V. Palomares, P. Serras, I. Villaluenga, K.B. Hueso, J. Carretero-Gonzalez, T. Rojo, Na-ion batteries, recent advances and present challenges to become low cost energy storage systems, Energy and Environmental Science 5 (2012) 5884.
[5] L.W. Shacklette, T.R. Jew, L. Townsend, Rechargeable electrodes from sodium cobalt bronzes, Journal of the Electrochemical Society 135 (1988) 2669.
[6] S. Bach, J.P. Pereira-Ramos, P. Willmann, A sodium layered manganese oxides as 3 V cathode materials for secondary lithium batteries, Electrochimica Acta 52 (2006) 504.
[7] S. Komaba, C. Takei, T. Nakayama, A. Ogata, N. Yabuuchi, Electrochemical intercalation activity of layered $NaCrO_2$ vs. $LiCrO_2$, Electrochemistry Communications 12 (2010) 355.
[8] S. Okada, Y. Takahashi, T. Kiyabu, T. Doi, J.I. Yamaki, T. Nishida, Layered transition metal oxides as cathodes for sodium secondary battery, in: 210th ECS Meeting Abstract B2, 2006, p. 201.
[9] J.J. Braconnier, C. Delmas, C. Fouassier, P. Hagenmuller, Comportement electrochimique des phases Na_xCoO_2, Materials Research Bulletin 15 (1980) 1797.
[10] S. Miyazaki, S. Kikkawa, M. Koizumi, Chemical and electrochemical deintercalations of the layered compounds $LiMO_2$ (M = Cr, Co) and $NaM'O_2$ (M′ = Cr, Fe, Co, Ni), Synthetic Metals 6 (1983) 211.
[11] X. Xin, J.R. Dahn, A study of the reactivity of deintercalated P_2-Na_xCoO_2 with nonaqueous solvent and electrolyte by accelerating rate calorimetry, Journal of the Electrochemical Society 159 (2012) A647.
[12] N. Yabuuchi, M. Kajiyama, J. Iwatat, H. Nishikawa, S. Hitomi, R. Okuyama, R. Usui, Y. Yamada, S. Komaba, P2-type $Na_x[Fe_{1/2}Mn_{1/2}]O_2$ made from earth-abundant elements for rechargeable Na batteries., Nature Materials 11 (2012) 512.
[13] D. Kim, S.-H. kang, M. Slater, S. Rood, J.T. Vaughey, N. Karan, M. Balasubramanian, C.S. Johnson, Enabling sodium batteries using lithium-substituted sodium layered transition metal oxide cathodes, Advanced Energy Materials 1 (2011) 333.
[14] Q. Huang, M.L. Foo, R.A. Pascal Jr., J.W. Lynn, B.H. Toby, T. He, H.W. Zandbergen, R.J. Cava, Coupling between electronic and structural degrees of freedom in the triangular lattice conductor Na_xCoO_2, Physical Review B 70 (2004) 184110.
[15] D. Carlier, M. Blangero, M. Menetrier, M. Pollet, J-P. Doumerc, C. Delmas, Sodium ion mobility in Na_xCoO_2 ($0.6 < x < 0.75$) cobaltites studied by ^{23}Na MAS NMR, Inorganic Chemistry 48 (2009) 7018.
[16] R. Berthelot, D. Carlier, C. Delmas, Electrochemical investigation of the P2-Na_xCoO_2 phase diagram, Nature Materials 10 (2011) 74.
[17] R.J. Balsys, R.L. Davis, Refinement of the structure of $Na_{0.74}CoO_2$ using neutron powder diffraction, Solid State Ionics 93 (1996) 279.
[18] Y. Ono, R. Ishikawa, Y. Miyazaki, Y. Ishii, Y. Morii, T. Kajitani, Crystal structure, electric and magnetic properties of layered cobaltite β-Na_xCoO_2, Journal of Solid State Chemistry 166 (2002) 177.
[19] L. Viciu, J.W.G. Bos, H.W. Zandbergen, Q. Huang, M.L. Foo, S. Ishiwata, A.P. Ramirez, M. Lee, N.P. Ong, R.J. Cava, Crystal structure and elementary properties of Na_xCoO_2 ($x = 0.32$, 0.51, 0.6, 0.75, and 0.92) in the three-layer $NaCoO_2$ family, Physical Review B 73 (2006) 174104.
[20] Y.S. Meng, Y. Hinuma, G. Ceder, An investigation of the sodium patterning in Na_xCoO_2 ($0.5 < x < 1$) by density functional theory methods, Journal of Chemical Physics 128 (2008) 104708.
[21] G. Lang, J. Bobroff, H. Alloul, G. Collin, N. Blanchard, Spin correlations and cobalt charge states: Phase diagram of sodium cobaltates, Physical Review B 78 (2008) 155116.
[22] F.T. Huang, M.W. Chu, G.J. Shu, H.S. Sheu, C.H. Chen, L.K. Liu, P.A. Lee, F.C. Chou, X-ray and electron diffraction studies of superlattices and long-range three-dimensional Na ordering in γ-Na_xCoO_2 ($x = 0.71$ and 0.84), Physical Review B 79 (2009) 014413.
[23] M. D'Arienzo, R. Ruffo, R. Scotti, F. Morazzoni, C.M. Mari, S. Polizzi, Layered $Na_{0.71}CoO_2$: a powerfull candidate for viable and high perfomance Na-batteries, Physical Chemistry Chemical Physics 14 (2012) 5945.
[24] Z.H. Chen, J.R. Dahn, Improving the capacity retention of $LiCoO_2$ cycled to 4.5 V by heat-treatment, Electrochemical and Solid-State Letters 7 (2004) A11.
[25] C. Vidal-Abarca, P. Lavela, J.L. Tirado, A.V. Chadwick, M. Alfredsson, E. Kelder, Improving the cyclability of sodium-ion cathodes by selection of electrolyte solvent, Journal of Power Sources 197 (2012) 314.
[26] A. Ponrouch, E. Marchante, M. Courty, J.-M. Tarascon, M.R. Palacin, In search of an optimized electrolyte for Na-ion batteries, Energy and Environmental Science 5 (2012) 8572.
[27] J. Moulder, W. Stickie, P. Sobal, K. Bomber, Handbook of X-ray Photoelectron Spectroscopy, Perkin Elmer, Eden Prairie, 1992, p. 82.
[28] A. Deb, U. Bergmann, S.P. Cramer, E.J. Cairns, *In situ* X-ray absorption spectroscopic study of the $Li[Ni_{1/3}Co_{1/3}Mn_{1/3}]O_2$ cathode material, Journal of Applied Physics 97 (2005) 113523.
[29] I. Nakai, K. Takahashi, Y. Shiraishi, T. Nakagome, F. Nishikawa, Study of the Jahn-Teller distortion in $LiNiO_2$, a cathode material in a rechargeable lithium battery, by *in situ* X-ray absorption fine structure analysis, Journal of Solid State Chemistry 140 (1998) 145.